

Research Article

Natural flavonoid pectolinarin computationally targeted as a promising drug candidate against SARS-CoV-2

Mukta Rani^{a,**,1}, Amit Kumar Sharma^{b,***,1}, R.S. Chouhan^c, Souvik Sur^d, Rani Mansuri^e, Rajesh K. Singh^{f,*}^a National Institute for Plant Biotechnology, Indian Council of Agricultural Research, Pusa Campus, New Delhi, 110012, India^b Department of Physics, Faculty of Engineering, Teerthanker Mahaveer University, Moradabad, 244001, U.P, India^c Department of Environmental Sciences, Jozef Stefan Institute, Jamova Cesta-39, Ljubljana, Slovenia^d Research and Development Center, Teerthanker Mahaveer University, Moradabad, 244001, U.P, India^e School of Pharmaceutical Sciences, Apeejay Stya University, Gurugram, Haryana, 122103, India^f Department of Pharmaceutical Chemistry, Shivalik College of Pharmacy, Nangal, District Ropar, Punjab, 140126, India

ARTICLE INFO

Handling editor: N Strynadka

Keywords:

Coronaviruses

SARS-CoV2

S-glycoproteins

Motif

Computational analysis

ABSTRACT

Coronavirus disease-2019 (COVID-19) has become a global pandemic, necessitating the development of new medicines. In this investigation, we identified potential natural flavonoids and compared their inhibitory activity against spike glycoprotein, which is a target of SARS-CoV-2 and SARS-CoV. The target site for the interaction of new inhibitors for the treatment of SARS-CoV-2 has 82% sequence identity and the remaining 18% dissimilarities in RBD S1-subunit, S2-subunit, and 2.5% others. Molecular docking was employed to analyse the various binding processes used by each ligand in a library of 85 natural flavonoids that act as anti-viral medications and FDA authorised treatments for COVID-19. In the binding pocket of the target active site, remdesivir has less binding interaction than pectolinarin, according to the docking analysis. Pectolinarin is a natural flavonoid isolated from *Cirsiumsetidensas* that has anti-cancer, vasorelaxant, anti-inflammatory, hepatoprotective, anti-diabetic, anti-microbial, and anti-oxidant properties. The S-glycoprotein RBD region (330–583) is inhibited by kaempferol, rhoifolin, and herbacetin, but the S2 subunit (686–1270) is inhibited by pectolinarin, morin, and remdesivir. MD simulation analysis of S-glycoprotein of SARS-CoV-2 with pectolinarin complex at 100ns based on high dock-score. Finally, ADMET analysis was used to validate the proposed compounds with the highest binding energy.

1. Introduction

Coronaviruses (CoVs) were first time found in 1960s and have the largest RNA genome. They were kept in the largest family of Nidovirales (Ashour et al., 2020). Now days, the humankind wide scientific interest on CoVs first time known after the emergence of Severe Acute Respiratory Syndrome coronavirus (SARS-CoV) raised in 2002–2003 tracked by Middle East Respiratory Syndrome CoV (MERS-CoV) in China (Walls et al., 2020). In current, the second cycle of first CoV emerged from Wuhan, China called 2019-nCoV (i.e. SARS-CoV-2 or COVID-19) as an unexplained case of pneumonia on Dec 31, 2019 after that on Jan 30, 2020, WHO declared the outbreak of COVID-19 as Public Health

Emergency of International Concern. Further, the family of Coronaviridae was classified into two subfamilies like *Orthocoronavirinae* and *Torovirinae*. Further, the ortho-coronavirinae having four genera: α -CoV, β -CoV, γ -CoV, and δ -CoV. CoVs are generally originated from mammals and birds and also common in cats, bats, camels, and other animals. But rarely, animal CoVs have the capacity to infect humans and could further spread through human-to-human transmission (Forni et al., 2017). As on September 6th 2023, WHO has reported a total of confirmed cases 770, 437, 327 of SARS-CoV-2 cases and 6,956,900 deaths in worldwide (WHO, 2020). On the rise cases day by day, worldwide scientific interest indicate that this outbreak as one of the worst pandemics. Scientists are looking for cutting-edge treatment

* Corresponding author.

** Corresponding author.

*** Corresponding author.

E-mail addresses: mukta.rani1@gmail.com (M. Rani), amit.db1980@gmail.com (A.K. Sharma), rksingh244@gmail.com (R.K. Singh).¹ Dr. Mukta Rani and Dr. Amit Kumar Sharma and Dr. Rajesh K. Singh contribute equally.<https://doi.org/10.1016/j.crstbi.2023.100120>

Received 19 September 2023; Received in revised form 11 December 2023; Accepted 11 December 2023

Available online 15 December 2023

2665-928X/© 2023 The Authors. Published by Elsevier B.V. This is an open access article under the CC BY-NC-ND license (<http://creativecommons.org/licenses/by-nc-nd/4.0/>).

approaches to fight COVID-19 infection (Rabie and Abdalla, 2022; Eltayb et al., 2023; Rabie, 2021). But at present, there are no suitable drugs or therapies against SARS-CoV-2.

SARS-CoV-2 is a single-stranded RNA virus which belongs to the subgenus β -CoVs. Recently, scientific reports suggest that the SARS-CoV-2 binds to the human ACE-2 receptor through densely transmembrane spike (S) glycoprotein (S-glycoprotein) as the opening step of the way in mechanism to human cells (Hoffmann et al., 2020). These transmembrane S-glycoprotein arrangements are in homotrimers overhang from the viral surface (Tortorici and Veesler, 2019). It consists of two functional subunits bind to the host cell receptor (S1 subunit; 14–685 including NTD and RBD) and fusion of the epidemiologic and cellular membranes (S2 subunit; 686–1270) including calcium-dependent calmodulin binding, baculovirus polyhedron envelope protein, retroviral envelope protein known as GP4. In this study, the MukF_M domain is discovered and first time reported.

Drug-design employing natural substances has advanced rapidly in the previous two decades (Mehta et al., 2021a; 2021b). Natural products can provide effective antiviral activity against SARS-CoV-2 (Rabie, 2022). Flavonoids are natural substances with variable phenolic structures having 4000 identified kinds of flavonoids (Groot and Rauhen, 1998) and hold a range of favourable biochemical and antioxidant effects associated with a variety of diseases (Burak and Imen, 1999). Albert Szent-Gyorgyi reported the first evidence of biological activity of flavonoids in 1938 (Narayana et al., 2001). Widely use of flavonoids in biological activities such as antiviral, anticancer, anti-inflammatory, antioxidant, neuroprotective and antibacterial has been illustrated (Xia et al., 2010; Khan et al., 2013; Nabavi et al., 2015; Alzaabi et al., 2022).

To my knowledge, no structured evidence-based or clinical research have been reported that pectolinarin is the best suited natural inhibitors against the treatment of SARS-CoV-2, only reported that effective inhibitory activity against SARS-CoV-2 3CLpro with pectolinarin (Jo et al., 2020). We used molecular docking with PubChem compound search as natural flavonoids that serve as anti-viral medications in this study. A library of 85 compounds and FDA authorised treatments for COVID-19 were evaluated against S protein of SARS-CoV-2 and SARS-CoV. As a result, we noticed that the top five flavonoids and five FDA-approved medications are directed at the 3D structure of S-glycoprotein (in S1 and S2 subunits). This study also recommended that finding a suitable inhibitor for S-glycoprotein demonstrates that S1 subunits have very little interaction in the RBD area (330–583) but have a significant interaction with S2 subunit (686–1270) in the fusing of the epidemiologic and cellular membranes regions from pharmacological library. Furthermore, the S1 and S2 subunits of S-glycoprotein were docked and analysed, and it is found that flavonoids may play an important role in SARS-CoV-2 inhibitor.

2. Material and methods

The sequence of spike glycoprotein [Severe acute respiratory syndrome coronavirus 2] coded as S-glycoprotein in SARS-CoV-2 is published in March 18, 2020, which has composed of 1273 amino acid is retrieved from NCBI (GenBankID: QHD43416.1). Another sequence of spike protein [SARS coronavirus ZJ0301] coded as SARS-CoV, which was first reported in September 15, 2005 by Li et al. (2005). The source of this virus in vero cell was taken from throat swab from the first patient with severe acute respiratory syndrome (SARS) in Zhejiang, China, which has 1255 amino acid. The comparison study included retrieval of the 3D structure of S-glycoprotein in SARS-CoV-2 and SARS-CoV are the targets for further analysis. The anti-viral flavonoids and FDA approved drugs as treatment for infected peoples by COVID-19, their PDB structure are downloaded from PubChem compound search of NCBI. The 3Dstructure of these two target proteins was predicted by homology modelling and validated thorough RAMPAGE server (Lovell et al., 2003). Docking was performed by PatchDock and FireDock server and

whereas results of these docking complexes were visualized by Protein-Ligand Interaction Profiler (PLIP) server (Salentin et al., 2015). The ADMET properties was analysed through admetSAR server (Yang et al., 2019). Further, The best docked molecules with the highest binding energy with S-glycoprotein of SARS-CoV-2 with pectolinarin were chosen for molecular dynamics analysis using the AMBER22 software (Salomon-Ferrer et al., 2013; Case et al., 2005).

2.1. Sequence retrieval, homology modeling and validation

The sequence of S-glycoprotein in SARS-CoV-2 has 1273 amino acid are modelled through SwissModel (Waterhouse et al., 2018). The 3Dstructure which lays A27-D1146 amino acids, with sequence identity 97.39% with QMEAN is -2.60 . The modelled structure does not contain total 1273 amino acids for which we further modelled through the I-Tasser (Yang et al., 2015) and Phyre2 server (Kelley et al., 2015). The 3D modelled structure of SARS-CoV-2 and SARS-CoV were built by using as template the prefusion structure of SARS-CoV spike glycoprotein, conformation 2 (PDBID: 5 × 5B) (Yuan et al., 2017) and SARS-CoV complex with human neutralizing S230 antibody Fab fragment (PDBID: 6NB6) (Walls et al., 2019) with a sequence identity 64% and 84% respectively. The criteria for selection of the best 3Dstructures were predicted by using PDB advance BLAST analysis and the structures used in further analysis were those showing extreme score and query coverage (Rani et al., 2013). The homology of SARS-CoV-2 and SARS-CoV structures and their comparison are listed in Supplementary Table 1. The analysis of conformational accuracy and consistency approved by using Ramachandran plot by PROCHECK (Laskowski et al., 1993). The predicted SARS-CoV-2 and SARS-CoV model was validated using RAMPAGE (Lovell et al., 2003) and refined through protein structure refinement server is 3D-refine (Bhattacharya et al., 2016). The correct resolution of SARS-CoV and SARS-CoV-2 was visualized by using PyMOL (DeLano, 2002) and DiscoveryStudio3.0.

2.2. Molecular docking with flavonoids and FDA approved drugs

The modelled structure of SARS-CoV-2 and SARS-CoV were further used for *in-silico* docking analysis to understand the interaction between the anti-viral flavonoids and FDA approved drugs as treatment for COVID-19. The different methods applied in this research study are given below.

2.2.1. Preparation of proteins

Prior to docking, we employed an online tool named prepare PDB file for docking programs of WHATIF server for validate modelled 3Dstructure of SARS-CoV-2 and SARS-CoV. It was prepared the missing side chains in target 3Dstructure, small regularisation were performed, water positions modification, symmetry related waters and hydrogens are added if still needed by target proteins.

2.2.2. Preparation of ligands

Library of 85 natural flavonoids that serve as an anti-viral drugs and FDA approved drugs for COVID-19 were screened against S-glycoprotein of SARS-CoV-2 and SARS-CoV. The 3Dstructure of library including anti-viral flavonoids and FDA approved drugs are downloaded from Pubchem compound search of NCBI. The structures were downloaded as *.sdf file format and open through DSv3.0 visualization tool and converted into *.pdb file.

2.2.3. Docking analysis

The modelled 3D-structure of SARS-CoV-2 and SARS-CoV were used for protein-ligand interaction analysis by PatchDock (Schneidman-Duhovny et al., 2005), where entrant solutions shaped by rigid-body docking methods. The Clustering RMSD was 4.0 Å for analysis. The PatchDock algorithm divides Connolly dot surface that represent the molecules into convex, concave, and flat patches. These are harmonized

to create entrant transformations. Further, it was evaluated by scoring role that reflects both atomic de-solvation and geometric energy. It gives 1000 best docked transforms from PatchDock and output is obtained in terms of global energy, attractive repulsive van der Waals interactions, partial electrostatics, atomic contact energy (ACE) and further additional estimations of the binding free energy were further processed in FireDock server (Mashiach et al., 2008). FireDock re-scored the best 10 highest solutions by limiting the flexibility to the side-chains of the interrelating surface and permitting small rigid-body actions. This study was carried out by selecting the first best candidate solution from FireDock were retained. The results of these docking complexes were visualized by Protein-Ligand Interaction Profiler (PLIP) server. PyMol V2.0.7 and also through DSv3.0 visualizer and compare their result analysis.

2.3. Molecular dynamics study

The best docked molecules which have the highest binding energy with S-glycoprotein of SARS-CoV-2 with pectolarin obtained from the docking analysis were considered for molecular dynamics analysis by AMBER22 package (Salomon-Ferrer et al., 2013; Case et al., 2005). Molecular dynamics simulation offers the prospect of detailed description of the dynamic structure of ions and water at the molecular level. All the parameters were generated using literature values using the GAUSSIAN 03 and parameters were obtained using the restrained electrostatic potential (RESP) method of AMBER 22. The most effective force-field for our target SARS-CoV-2 was taken as ff19SB (Tian et al., 2020).

2.4. ADMET analysis

The ADMET features of the best interacted drug were further examined using the admetSAR server (Yang et al., 2019), with nitrogen-containing heterocyclic compounds previously reported with SARS-CoV-2 RdRp protein (Rabie et al., 2023).

3. Results

3.1. Sequence retrieval, homology modelling and validation

The modelled 3D structure of SARS-CoV-2 and SARS-CoV were built by using PDBID: 5X58_A and PDBID: 6NB6 as templates having identity 1 and identity 2 score is 0.77 and 0.64 and 1.00 and 0.84 respectively are shown in Supplementary Table 1. The coverage score is 0.83 (83%) in SARS-CoV-2 and 0.84 (84%) in SARS-CoV and the normalized Z-score is 4.27 and 4.28, it shows the good alignment between the query and templates (Z-score >1 normalized mean having good alignment). After that homology modelling followed by the validation by using 3Drefine and RAMPAGE web servers, which shows the five distinguished model structure and the top (model 5) have the best refined score is 79742.0. It is the possible energy of the improved model after using 3Drefine force field (a lower score indicates a higher quality model) and 'MolProbity score' is 3.591 gives the central MolProbity protein quality statistics as a single number and similarly in SARS-CoV has best refined score is 71805.0 and mol-probability score 3.344. The refined 3D model further get validated showed that 91.8% of the total residues found in the favoured region, 9.1% of the residues found in the allowed region and none of the residues were located in the disallowed region in Ramachandran plot. This results confirmed that the protein backbone dihedral angles phi (Φ) and psi (Ψ) occupied reasonably accurate positions in the built 3D model of SARS-CoV-2 and in 88.4% residues in the favoured region and 9.6% residues in allowed region (Supplementary Table 1). The C-score is a confidence score for assessing the value of predicted models by I-TASSER is -1.52 for SARS-CoV-2 and -1.0 for SARS-CoV. The TM-score is 0.825 in SARS-CoV-2 and 0.831 for SARS-CoV, it is a unit for calculating the similarity of two protein structures with RMSD score is 0.76 and 1.14. Since the experimental structure covers only 75% of the

residues in the full-length sequence, based on the available templates by I-TASSER and Phyre2, it was possible to model total 1273 amino acids length from Met¹ to Thr¹²⁷³ in SARS-CoV-2 and in SARS-CoV, Met¹ to Thr¹²⁵⁵. Thus, the above mentioned results of different scoring function showed that the modelled 3D structure of target proteins are the best fit for further study.

3.2. Structural and functional analysis

After modelling and validation we analysed structural and functional analysis of S-glycoprotein SARS-CoV-2 and SARS-CoV found that 4 transmembrane helices (TMH) from N-C terminal end i.e. L¹¹⁸-C¹³⁶, E²²⁴-L²⁴¹, Y⁸⁷³-F⁸⁸⁸ and Y¹²¹⁵-K¹²⁴⁵ and their number of residues are 19, 18, 16 and 31 amino acids (aas) in other K²¹⁷-A²³³, D²⁴³-L²⁶⁴, A⁸⁵⁷-G⁸⁷³ and Y¹¹⁹⁷-K¹²²⁷ and their residues ranges are 17, 22, 17 and 31 aas respectively. However result explains that the same number of TMHs is present but their position and residues were different. It means that the last TM helix is long (31aa) and present in both target proteins to facilitate the function as gateways to permit the transport of specific substances across the membranes. The N-terminal signal peptide in SARS-CoV-2 has M¹-R²¹ and in SARS-CoV M¹-V²⁴ has revealed the starting lipoprotein signal peptide (Lsp), which is involved in protein transport across different membrane cellular compartments or protein secretion from the cell (Parker, 2001). Interestingly, we found that in SARS-CoV-2 have eight protein families and their residues from N to C-terminal end comprises spike corona S1_subunit (14–685), N-terminal domain (262–294), spike receptor-binding domain (330–583), corona_S2 subunit (686–1270), calcium-dependent calmodulin binding (853–871), Baculovirus polyhedron envelope protein (925–988), Tetramerisation domain of TRPM (934–962) and retroviral envelope protein known as GP41 (1149–1241) are shown in Fig. 1. The GP41 family includes envelope protein from variety of retroviruses, similar in HIV and SIV (RNA as a genetic material) (Malashkevich et al., 1998). It mediates membrane fusion during viral entry into the host i.e. human. Likewise, we reported first time, that one protein families named as MukF_M (906–969) is present in SARS-CoV-2. A MukF_M domain is the middle coiled-coil domain of MukF and it plays significant role in chromosome segregation, condensation and cell cycle progression (Fennell-Fezzie et al., 2005). All these above mentioned five domains are mostly comprises in S2 subunit (686–1270) of spike protein, so this domain may play an important role in protein-ligand interaction analysis.

3.3. Molecular docking

After structural and functional analysis, we further used 3D model structure of SARS-CoV-2 and SARS-CoV for virtual screening with anti-viral flavonoids and FDA approved drugs and their analogues which are used as treatment on COVID-19 infected patients. By Sharma et al., (2011), protein-ligand interaction represents the numerical calculation of the most likely spatial positioning of interacting molecules, which are predominantly protein and tiny ligands. Prior to docking analysis, the PDB file for docking was prepared, which involved refining the missing side chains, adding or correcting water positions, and adding hydrogens as needed to make the protein more stable, behave more like a natural protein, and optimize its interaction with ligands. Various parameters were considered to calculate possibility of protein-ligand interaction were analysed by PatchDock server and their resultant transformations were refined through FireDock tool. But till date, there is no report about the interaction of S-glycoprotein of SARS-CoV-2 and SARS-CoV with FDA approved drugs like remdesivir (coded as Rd), chloroquine (coded as Cq), hydroxychloroquine (coded as HCq) are anti-malarial drugs and their analogues like hydroxychloroquine-sulfate (coded as HCS) and chloroquine-phosphate (coded as CqP). This study compiled the information on the interaction of the S-glycoprotein with the anti-viral flavonoids and FDA approved drugs with SARS-CoV-2 and SARS-CoV. It

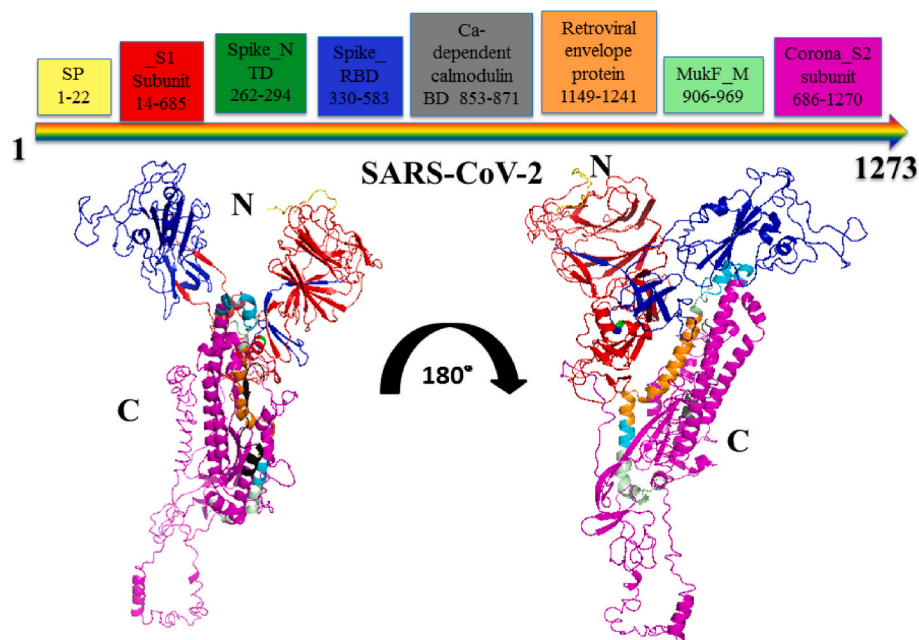


Fig. 1. 3D model structure of SARS-CoV2 and their different domains:

It is the schematic representation of S glycoprotein of SARS-CoV2 3D model structure and their different domains. Domains are arranged from N-terminal to C-terminal were colored coded in line representation is same in 3D model structure. This picture was generated by the PyMOL.

may provide a drug repositioning therapeutics and major target for further in-vitro and in-vivo analysis.

3.4. Docking result with flavonoids

Receptor-ligand interactions i.e. docking plays a significant role in all biological processes, is an essential tool in computer assisted drug design, in which a new drug have to fit the binding site of a target molecules. Different types of binding interaction like H-bond, hydrophobic, van der Waals interactions, salt-bridges and π -stacking interactions etc (Chen et al., 2016). To explore the different binding approaches of each ligand, molecular docking was carried out with PubChem compound search as natural flavonoids that acts as anti-viral drugs library of 85 compounds and FDA approved drugs on COVID-19 were screened against S-glycoprotein of SARS-CoV-2 and SARS-CoV. We listed the top five natural flavonoids and top five currently used FDA approved drugs, which have the highest binding affinities with both target proteins were summarized in Table 1. The binding energy or global energy (Kcal/mol) allows us to find the best result and compare on the basis of their binding affinity between different compounds (i.e. ligands) with their corresponding receptor molecule (i.e. target). A lower global energy indicates a higher binding affinity between ligand and receptor, ligands with the highest binding affinities may be selected as possible therapeutic candidates for further studies. The prominent binding sites in SARS-CoV-2 were predicted through COACH server (Yang et al., 2013) are L303, E309, K310, I312, Y313, E725, I726, L727, P728, N907, G946, K947, D950, N953, Q957, S1021, L1024, A1028, Q1036 and S1037. The spike glycoprotein in SARS-CoV-2 is surface glycoprotein of 2019 novel corona virus (nCoV), it plays significant roles during viral attachment, fusion and entry into the host cells i.e. human (Li, 2016). As a result that the top 5 natural flavonoids which shows the highest binding affinity with S-glycoprotein of SARS-CoV-2 were listed in Table 1 and found that pectolinarin have the highest binding affinity having global energy is -53.91 kcal/mol, attractive VdW is -30.85 kcal/mol, repulsive VdW is 8.38 kcal/mol and atomic contact energy (ACE) is -9.02 kcal/mol. Pectolinarin was isolated from *Cirsiumsetidens* and it is a bioactive phytochemical flavonoid have anti-microbial, anti-diabetic, anti-oxidant, anti-inflammatory, vasorelaxant,

hepatoprotective, and anti-cancer properties (Cho et al., 2016). However in case of FDA approved drugs, remdesivir have the highest global energy is -46.03 kcal/mol, attractive VdW is -29.89 kcal/mol, repulsive VdW is 17.13 and atomic contact energy (ACE) is -10.48 kcal/mol. Remdesivir is an adenosine analogue and anti-viral drug against RNA viruses (same as SARS-CoV/MERS-CoV) infection which incorporate into promising viral RNA chains and results in pre-mature termination (Sheahan et al., 2017). It is currently under clinical development against SARS-CoV-2. Simultaneously, morin have the lowest global energy is -39.64 kcal/mol and in FDA approved it shows the CqP have the lowest is -34.20 kcal/mol. Although in case of S-glycoprotein of SARS-CoV, herbacetin have highest binding energy is -53.12 kcal/mol, attractive VdW is -21.64 kcal/mol, repulsive VdW is 5.68 kcal/mol and ACE is -16.58 kcal/mol whereas in FDA approved drug, Cq was highest binding energy -50.41 kcal/mol, attractive VdW is -19.45 kcal/mol, repulsive VdW is 7.55 kcal/mol and ACE is -17.77 kcal/mol (Table 1).

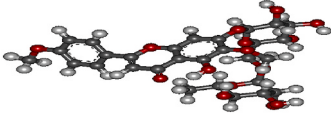
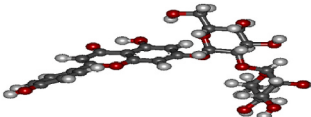
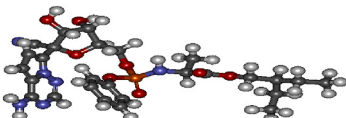
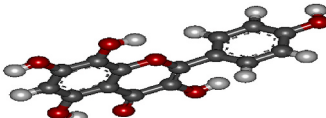
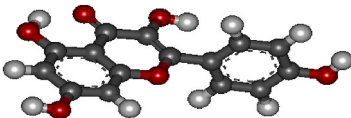
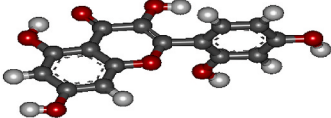
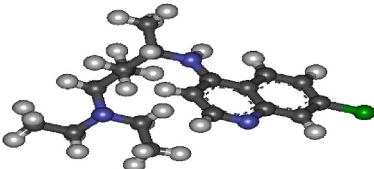
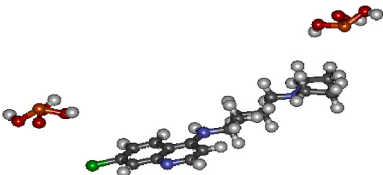
Morozov et al. (2004) define a hydrogen bond as an electrostatic interaction between an electronegative acceptor atom and a hydrogen atom covalently bound to an electronegative donor. The presence of hydrogen bonds between ligand and target underlines the importance of H-bonding for assessing protein structure and binding choice. The results revealed that the presence of highest number of H-bond i.e.6 and the interacted residues are GLU1092, ASN1108, TYR1209, LYS1211 and TRP1212 (S2 subunit) is found between natural flavonoid pectolinarin with S-glycoprotein of SARS-CoV-2 are shown in Fig. 2 and detailed information are shown Table 2 (Graphical abstract). The least number i.e.1 H-bond is present in interaction with kaempferol and residue is THR573, is hotspot point that lies in RBD of the S-glycoprotein of SARS-CoV-2. Interestingly, in FDA approved drugs remdesivir have revealed the highest, 3 H-bonding with involved amino acids are ASN907, THR912 and GLN1113 which lies in S2 subunit represented in Fig. 3.

One most important quality that we found in docking analysis of target with flavonoids, that only pectolinarin have revealed the two salt-bridges between ARG1107 and LYS1211 with 4.94 Å and 4.25 Å bond length detailed shown in Table 3 (Fig. 2). A non-covalent contact that results in two ionized sites is called a salt bridge. Salt bridges are strongest bond among all non-covalent interactions. A proton migrates

Table 1

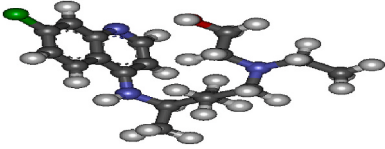
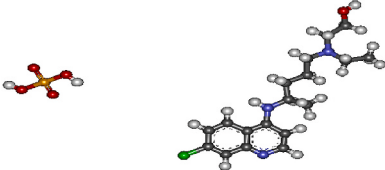
List of anti-viral flavonoids and FDA approved drugs

List of anti-viral flavonoids and FDA approved drugs for treatment of COVID-19 patients used for protein-ligand interaction analysis. In 3D structure red colour code for oxygen, grey code carbon, purple code nitrogen, white code hydrogen, orange code phosphorus and green code chlorine, picture is generated by Discovery Studio.

	Flavonoids	Pubchem compound Ids:	3-D structure
1	Pectolinarin	CID_168849	
2	Rhoifolin	CID_5282150	
3	Remdesivir	CID_121304016	
4	Herbacetin	CID_5280544	
5	Kaempferol	CID_5280863	
6	Morin	CID_5281670	
FDA approved drugs:			
7	Chloroquine	CID_2719	
8	Chloroquinephosphate	CID_64927	

(continued on next page)

Table 1 (continued)

	Flavanoids	Pubchem compound Ids:	3-D structure
9	Hydroxychloroquine	CID_3652	
10	Hydroxychloroquinesulfate	CID_12947	

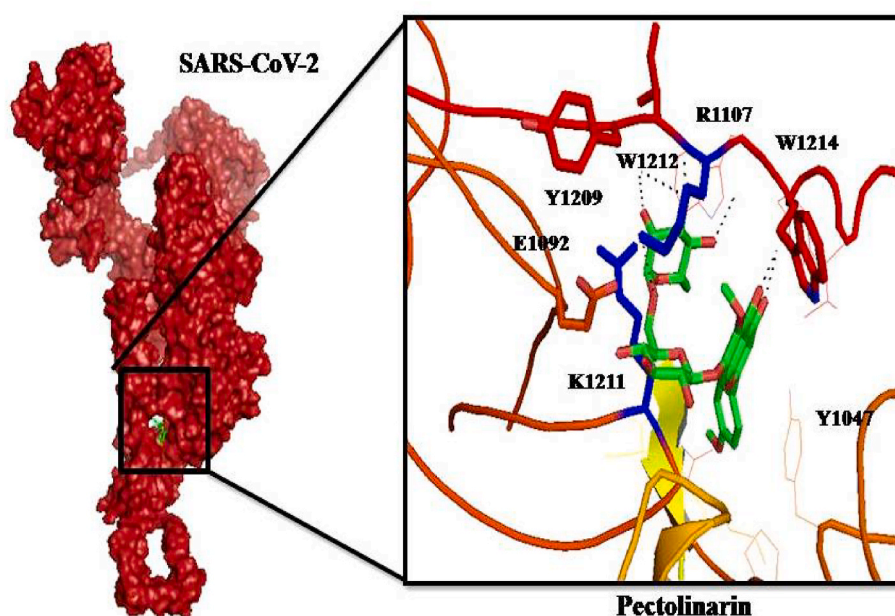


Fig. 2. Docking analysis of SARS-CoV-2 with pectolinarin

It shows the detailed view of docking analysis of S glycoprotein of SARS-CoV-2 with flavonoid pectolinarin shows the highest dock score is -51.91 and also highest number of H-bond is 6, protein shown in red color surface view. In box is the detailed view of protein represented in multicolour cartoon form and pectolinarin is represented in green and red color stick form is carbon and oxygen respectively. The S2 subunit of SARS-CoV2-SP (red stick) which involved in formation of 6 H-bonding with pectolinarin and blue stick is involved in formation of 2 salt bridges formation residues are R1107 and K1211. Picture is generated from PyMOL visualization tool. (For interpretation of the references to color in this figure legend, the reader is referred to the Web version of this article.)

(ligand atom: 9941, 9942) from $-HCOO$ group to $-NH$ or to the guanidine group in arginine in a salt-bridge. The salt bridges contain Lys or Arg as the bases so ARG1107 and LYS1211 are involved in formation of salt-bridge. Similarly, in chloroquine phosphate (FDA approved drug) one more salt-bridge is present with GLU484 is tertamine ligand group and ligand atom is 9951, and their bond length is 5.22 \AA shown in Table 3. However, pectolinarin with SARS-CoV-2 and herbacetin with SARS-CoV having the highest binding affinity, therefore we evaluate these flavonoids by different chemical ADMET properties, resulted to suggest that novel drugs for the treatment of COVID-19. The various key residues and their particular domain are revealed in graph, which is shown in graphical abstract.

3.5. Molecular dynamics analysis

The S-glycoprotein of SARS-CoV-2 with pectolinarin complex was subjected to 100 ns MD simulation to determine the interaction stability

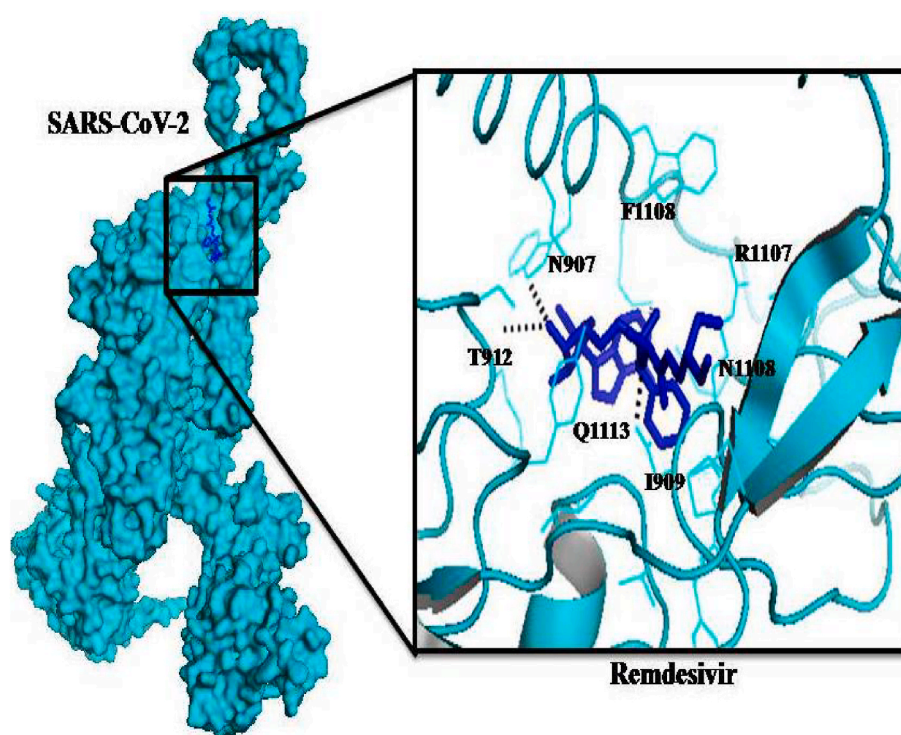
by AMBER22 package. The macroscopic parameters of the systems, such as pressure, temperature, volume, density, and others, remained constant across the 100ns MD simulation, indicating that the simulation was successful. The trajectory analysis revealed that the simulation procedure resulted in a stable structure. No major helical unfolding of SARS-CoV-2 protein structure was observed during the simulations. The root mean square deviation (RMSD) fluctuation during whole 100ns simulation time was reported in Fig. 4 and the RMSF (root mean square fluctuation) values of SARS-CoV-2 protein with pectolinarin, was plotted (Fig. 4, inset). To calculate RMSD values, 1000 frames from a 100 ns simulation of MD were chosen every 100 ps. Radius of gyration values were also determined from the MD trajectory in Fig. 5, The initial deviation was observed up to 55 ns simulation but after that the curve tends to be constant throughout rest of the simulation time which means the convergence of whole MD trajectory as we observed the ligand was effectively bound to SARS-CoV-2 model structure in the time averaged structure obtained from MD shown in Fig. 6. The pectolinarin binding

Table 2

Docking Score of SARS-CoV-2 and SARS-CoV with flavonoids and FDA approved drugs:

Comparative docking score of SARS-CoV-2 and SARS-CoV with anti-viral flavonoids and FDA approved drugs which are used as treatment on COVID-19 patients. Bold part shows the highest dock score with targets.

Sl No	SARS-CoV-2				SARS-CoV					
	Flavonoids (in order to highest score)	Global Energy (Kcal/mol)	Attractive VdW (Kcal/mol)	Repulsive VdW (Kcal/mol)	ACE (Kcal/mol)	Flavonoids (in order to highest score)	Global Energy (Kcal/mol)	Attractive VdW (Kcal/mol)	Repulsive VdW (Kcal/mol)	ACE (Kcal/mol)
1	Pectolinarin	-53.91	-30.85	8.38	-9.02	Herbactin	-53.12	-21.64	5.68	-16.58
2	Rhoifolin	-44.58	-20.64	4.48	-11.09	Morin	-52.33	-20.62	3.90	-16.22
3	Herbactin	-43.97	-17.27	3.40	-13.74	Rhoifolin	-48.91	-25.54	6.72	-12.24
4	Kaempferol	-43.89	-18.00	7.05	-15.1	Pectolinarin	-45.52	-21.43	5.70	-12.63
5	Morin	-39.64	-17.95	6.07	-11.42	Kaempferol	-41.58	-19.24	8.37	-12.97
FDA approved drugs on COVID-19 patients										
6	Remdesivir	-46.03	-29.89	17.13	-10.48	Chloroquine	-50.41	-19.45	7.55	-17.77
7	Hydroxychloroquine-sulfate	-43.37	-19.41	8.05	-16.04	Hydroxychloroquine	-48.38	-17.75	2.36	-16.05
8	Hydroxychloroquine	-36.52	-19.02	3.02	-6.69	Chloroquinephosphate	-46.83	-20.11	3.70	-12.94
9	Chloroquine	-35.48	-17.90	0.88	-5.95	Hydroxychloroquine-sulfate	-45.04	-17.67	4.45	-13.93
10	Chloroquinephosphate	-34.20	-19.41	4.54	-6.73	Remdesivir	-42.89	-23.23	6.66	-10.42

**Fig. 3.** Docking analysis of SARS-CoV-2 with remdesivir

It shows the full view of docking analysis of S glycoprotein of SARS-CoV-2 shown in cyan color (surface view) with FDA approved drug in COVID-19 patients as a treatment i.e. remdesivir shows the highest dock score is -46.03 in all FDA approved drug shown in blue color. In box is the detailed view of protein represented in cyan color cartoon form and remdesivir is represented in blue stick form respectively. The S2 subunit of SP-SARS-CoV2 is involved in formation of 3 H-bond with involved residues are N907, T912 and Q1113. Picture is generated from PyMOL visualization tool. (For interpretation of the references to color in this figure legend, the reader is referred to the Web version of this article.)

was adequately maintained throughout the simulation. The simulated protein-ligand structure revealed a set of conformation with a 7–10 RMSD.

3.6. ADMET (absorption, distribution, metabolism, excretion, and toxicity) analysis

ADMET are plays significant roles in drug designing (Singh et al.

2013, 2015). In this analysis, we predicted the different chemical ADMET properties of natural flavonoids which having the highest global energy i.e. pectolinarin with SARS-CoV-2 and herbactin with SARS-CoV (Table 4). The scoring role was well-defined on the basis of 27ADMET properties analysed through web server admetSAR. In this research study, we suggested a scoring function named the ADMET-score to estimate drug-likeness of natural flavonoid (for any ligands) like human intestinal absorption (HIA), blood-brain barrier

Table 3

Formation of H-bonding and involved residues.

Residues involve in formation of H-bonding with flavonoids and FDA approved drugs with SP in SARS-CoV-2. Table represents that drug name with number of H-bond and key residues of SP in SARS-CoV-2 along with the respective distances and bond angle and number of residues involved in formation of H-bond. H represents the hydrogen, A is acceptor and D is donor.

LIGAND/No of H-bond	Residue	Distance H-A (Å)	Distance D-A (Å)	Donor Donor Angle (Å)	Donor Atom	Acceptor Atom	Involved residues
1. Pectolinarin (6)	GLU 1092	2.02	2.66	122.28	9943 [O3]	8512 [O3]	5
	GLU 1092	1.8	2.63	145.01	8512 [O3]	9941 [O3]	
	ASN 1108	3.11	3.74	123.36	8644 [Nam]	9951 [O2]	
	TYR 1209	2.55	3.26	129.8	9948 [O3]	9443 [O2]	
	LYS 1211	3.23	3.99	134.87	9460 [Nam]	9947 [O3]	
	TRP 1212	1.95	2.51	114.57	9949 [O3]	9479 [N2]	
2. Rhoifolin (2)	GLY381	2.41	2.86	107.7	9943 [O3]	3062 [O2]	2
	LYS386	2.38	2.76	102.93	9948 [O3]	3098 [N3]	
3. Herbacetin (4)	GLU516	3.51	4.1	123.22	9945 [O3]	4131 [N2]	4
	ASN544	3.39	4.0	124.66	9942 [O3]	4348 [O2]	
	GLY545	2.84	3.32	112.74	9941 [O3]	4356 [O2]	
	GLN564	2.84	3.58	132.9	4504 [Nam]	9942 [O3]	
4. Kaempferol (1)	THR573	3.18	3.61	108.49	4572 [O3]	9945 [O3]	1
5. Morin (5)	MET 740	1.37	2.03	121.62	9946 [O3]	5810 [O2]	4
	VAL963	3.22	3.77	119.36	9945 [O3]	7512 [O2]	
	LEU977	2.0	2.48	107.6	7609 [Nam]	9943 [O2]	
	ARG1000	2.65	3.58	156.85	7800 [Ng+]	9941 [O3]	
	ARG1000	3.21	4.02	140.95	7801 [Ng+]	9941 [O3]	
FDA approved drugs on COVID-19 patients:							
6. Remdesivir (3)	ASN907	1.89	2.31	102.42	9954 [Npl]	7100 [O2]	3
	THR912	251	3.25	132.79	7130 [O3]	9952 [N1]	
	GLN1113	3.17	3.58	107.18	8692 [Nam]	9952 [N1]	
7. Hydroxychloroquine-sulfate (2)	VAL6	2.43	3.26	147.66	9951 [O3]	49 [O2]	2
	LEU10	2.73	3.68	163.17	76 [Nam]	9948 [O3]	
8. Hydroxychloroquine (0)	NO-H-bond						
9. Chloroquine (2)	ARG1107	2.27	2.63	100.25	8635[Ng+]	9943[Nar]	2
	ASN1108	2.93	3.89	167.41	8644 [Nam]	9941 [N3]	
10. Chloroquinephosphate(2)	GLU484	2.71	3.14	108.68	3877 [O3]	9952[Npl]	2
	ASN487	1.65	2.31	121.21	9949 [O3]	3900 [O2]	

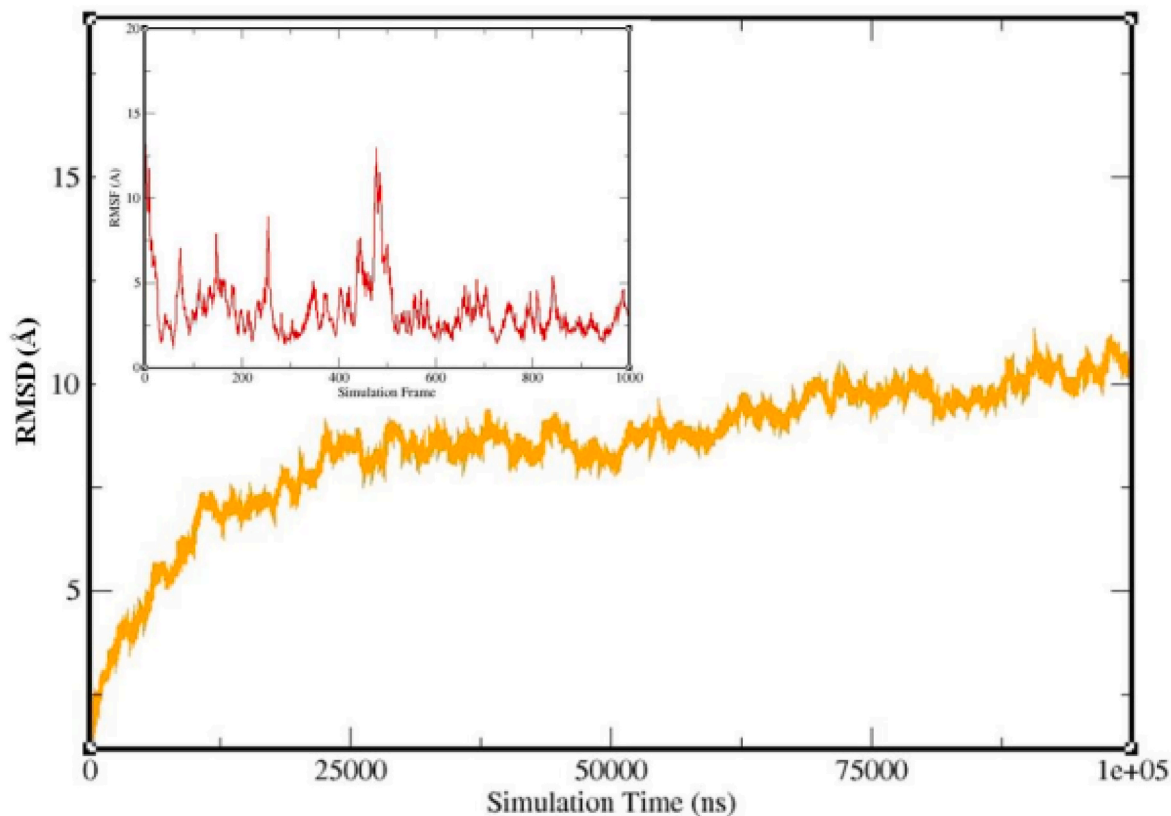


Fig. 4. Molecular dynamics simulation: Backbone RMSD of SARS-CoV-2. The yellow curve represents the backbone RMSDs for 100 ns simulations. The red curve represents the RMSF for the 100 ns MD simulation. (For interpretation of the references to color in this figure legend, the reader is referred to the Web version of this article.)

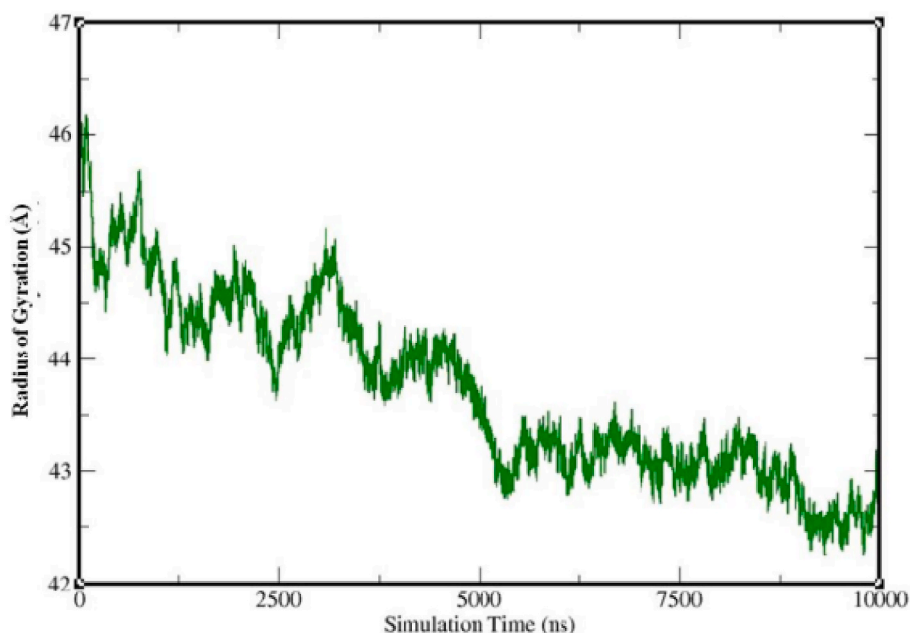


Fig. 5. Radius of gyration: The radius of gyration of the SARS-CoV-2-model backbone.

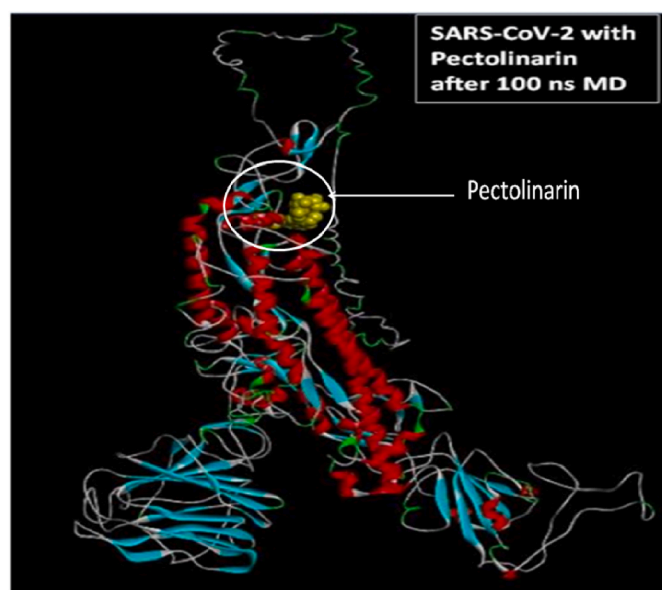


Fig. 6. Molecular dynamics simulation of S glycoprotein of SARS-CoV-2 with pectolinarin complex: It shows the time average structure of S glycoprotein of SARS-CoV-2 with pectolinarin complex.

(BBB), caco-2 permeability, aqueous solubility and toxicity. The sub-cellular localization of both ligands are in mitochondria are summarized in Table 5. Pectolinarin and herbacetin have non AMES toxic and

non-carcinogens properties, so it may be a novel therapeutic for COVID-19. According to these findings, the ADMET-score of pectolinarin and herbacetin would be a wide-ranging key to estimate biological drug-likeness. It would also assist researchers in choosing a suitable drug for SARS-CoV-2 during clinical examination.

4. Discussion

These results focus on the molecular modelling and docking of S-glycoprotein of SARS-CoV-2 and SARS-CoV and constructed a 3D model structure that provides insight into the protein's structure for promising interaction studies with our choice of inhibitors and binds to the possible important residues of S-glycoprotein that are essential in interaction with different flavonoids and inhibits viral entry into the cell and pathogenesis. Flavonoids with broad biological activity, such as antiviral activity and SARS viruses (Yang et al., 2013), were taken into account in this work. The modelled 3D structure of SARS-CoV-2 and SARS-CoV were built by using PDBID: 5X58_A and PDBID: 6NB6 have represented the coverage score is 0.83 (83%) in SARS-CoV-2 and 0.84 (84%) in SARS-CoV representing the total coverage of alignment equal to the number of aligned residues alienated by the length of the query protein. The 3D modelled structures were validated by using 3Drefine and RAMPAGE, which defines best refined score is 79742 and 71805 for SARS-CoV-2 and SARS-CoV respectively. Because the experimental structure only includes 75% of the full-length sequence's residues, based on the available templates by I-TASSER and Phyre2, it was possible to model total 1273 amino acids length from Met1 to Thr1273 in SARS-CoV-2 and in SARS-CoV from Met1 to Thr1255 were validate for further analysis.

In structure and functional analysis of S-glycoprotein SARS-CoV-2

Table 4

Formation of salt bridges:

Residues involve in formation of salt bridges with flavonoids and FDA approved drugs with SP in SARS-CoV-2.

S. No	Flavonoids	Aminoacids	Distance (Å)	Ligand groups	Ligand Atoms
1	Pectolinarin	ARG 1107	4.94	Carboxylate	9941, 9942
		LYS 1211	4.25	Carboxylate	9941, 9942
2	Chloroquinephosphate	GLU484	5.22	Tertamine	9951

Table 5

ADMET analysis

It shows the ADMET analysis of best interacted anti-viral flavonoids which having the highest global energy with SP-SARS-CoV-2 and SARS-CoV.

ADMET Predicted Profile — Classification		Target Drugs with Probability	
		Pectolinarin	Herbacetin
Absorption			
Blood-Brain Barrier	BBB-	0.9517	0.5711
Human Intestinal Absorption	HIA+	0.6118	0.965
Caco-2 Permeability	Caco 2-	0.8869	0.8957
P-glycoprotein Substrate	Substrate	0.6895	0.5629
P-glycoprotein Inhibitor-I	Non-inhibitor	0.8261	0.9297
P-glycoprotein Inhibitor-II	Non-inhibitor	0.7317	0.8382
Renal Organic Cation Transporter	Non-inhibitor	0.9086	0.931
ADMET Predicted Profile — Regression			
Aqueous solubility	LogS (unit)	-2.9062	-2.9994
Caco-2 Permeability	LogPapp, cm/s (unit)	-0.2724	0.2245
Distribution			
Subcellular localization	Mitochondria	0.668	0.5892
Metabolism			
CYP450 2C9 Substrate	Non-substrate	0.7975	0.7898
CYP450 2D6 Substrate	Non-substrate	0.9028	0.9116
CYP450 3A4 Substrate	Non-substrate	0.5684	0.653
CYP450 1A2 Inhibitor	Inhibitor	0.9113	0.9106
CYP450 2C9 Inhibitor	Non-inhibitor	0.9351	0.5823
CYP450 2D6 Inhibitor	Non-inhibitor	0.9356	0.9287
CYP450 2C19 Inhibitor	Non-inhibitor	0.9301	0.9025
CYP450 3A4 Inhibitor	Inhibitor	0.931	0.6951
CYP Inhibitory Promiscuity	High CYP Inhibitory Promiscuity	0.6965	0.5822
Excretion			
Toxicity			
Human Ether-a-go-go-Related Gene Inhibition	Weak inhibitor	0.9851	0.9781
	Non-inhibitor	0.786	0.8161
AMES Toxicity	Non AMES toxic	0.8959	0.722
Carcinogens	Non-carcinogens	0.9576	0.945
Fish Toxicity	High FHMT	0.858	0.9564
Tetrahymena Pyriformis Toxicity	High TPT	0.9972	0.9961
Honey Bee Toxicity	High HBT	0.702	0.633
Biodegradation	Not ready biodegradable	0.9342	0.8672
Acute Oral Toxicity	II	0.685	0.7348
Carcinogenicity (Three-class)	Non-required	0.6809	0.675
ADMET Predicted Profile — Regression			
Rat Acute Toxicity	LD50, mol/kg	2.7287	3.02
Fish Toxicity	PLC 50, mg/L	0.8594	0.4787
Tetrahymena Pyriformis Toxicity	pIGC50, ug/L	0.6919	0.6854

and SARS-CoV, found that 4 transmembrane helices (TMH), N-terminal signal peptide from M¹-R²¹ and M¹-V²⁴ has shown the starting lipoprotein signal peptide (Lsp), which involved in the transport to different membranous cellular compartments or secretion of the protein from the cell. Spontaneously, in SARS-CoV-2, eight different protein families and their residues from N-C terminal end comprises spike corona S1-subunit, spike RBD, corona-S2 subunit, calcium-dependent calmodulin binding, Baculovirus polyhedron envelope protein, tetramerisation domain of TRPM and retroviral envelope protein known as GP41 (Fig. 1). In this research hypothesis, we reported that the MukF_M protein family is present only in SARS-CoV-2, which shows the significant role in cell cycle progression, chromosome segregation and condensation process.

Docking analysis of S-glycoprotein of SARS-CoV-2 and SARS-CoV with anti-viral flavonoids and FDA approved drugs are carried through PatchDock and refined through FireDock server. As a result, we found that pectolinarin showed the best docking result with good binding energy in all other flavonoids under consideration indicating

their strong affinity against the S-protein of SARS-CoV-2. But in SARS-CoV shows better interaction with herbacetin have good binding energy in all other flavonoids. In case of FDA approved drugs on COVID-19 patients, remdesivir, and chloroquine showed that the highest global energy with SARS-CoV-2 and SARS-CoV respectively. Docking results thus indicated that in all total drugs and flavonoids, only pectolinarin have shows the highest binding energy i.e. 53.91 kcal/mol in SARS-CoV-2 with presence of 6-hydrogen bonding. All the ADMET parameters of those flavonoids that having the highest global energy i.e. pectolinarin with SARS-CoV-2 and herbacetin with SARS-CoV flavonoids were compared with the controls taken into consideration in this study. Successful molecular dynamics analysis of 100 ns showed that the best docked structure of pectolinarin was effectively bind to SARS-CoV-2 with optimum RMSD and RMSF values.

Overall study indicates towards pectolinarin (1108–1212) that can be isolated from *Cirsiumsetidensis* which is the best inhibitor for target in S2 subunit (686–1270) of spike protein and also works as an anti-diabetic, anti-microbial, anti-cancer, vasorelaxant, anti-inflammatory, hepatoprotective and anti-oxidant properties. While FDA approved drug remdesivir has found comparatively less binding interaction than pectolinarin. These docked results also clear that hydroxychloroquine does not have any interaction with S protein. This study also revealed that kaempferol, rhoifolin and herbacetin are inhibitor in the RBD region (330–583) while pectolinarin, morin, remdesivir, chloroquine, chloroquine phosphate are inhibitor in S2 subunit (686–1270) of spike protein where hydroxychloroquine-sulfate is an inhibitor of the signal peptide of spike protein.

5. Conclusion

In this conclusion, we found kaempferol, rhoifolin and herbacetin are inhibitor of RBD region (330–583) while pectolinarin, morin, remdesivir are inhibitor of S2-subunit (686–1270) of S-glycoprotein (Fig. Graphical abstract), and this interaction of S protein was exhibiting Signal peptide (SP), S1 (with component of RBD region), and S2 (MukF_M, BaPEP, and GP41) subunits of concern as common residues with novel results. The most H-bonds are found in Pectolinarin, and the interacting residues include GLU 1092, ASN 1108, TYR 1209, LYS 1211, and TRP 1212, which are found in the S2 subunit of SP-SARS-CoV-2. Based on high dock score, molecular dynamics simulation analysis of S glycoprotein of SARS-CoV-2 with pectolinarin complex at 100 ns takes places. As a result we found that the top first natural flavonoids i. e pectolinarin (SARS-CoV-2) and herbacetin (SARS-CoV) were subjected to ADMET analysis. The pharmacokinetics and ADMET (absorption/distribution/metabolism/excretion/toxicity; Table 5) analysis of the ligands pectolinarin and herbacetin reveals balanced and favourable drug-like behaviours those allow it to progress to the pharmacological and clinical phases for anti-viral drug therapeutics and drug development. Our finding shows that the pectolinarin may be well suited natural inhibitor against the treatment of SARS-CoV-2.

Pectolinarin inhibits S-glycoprotein S2-subunit (686–1270) (Fig. Graphical abstract), and this interaction of S protein revealed Signal peptide (SP), S1, and S2 subunits of concern as shared residues with innovative drug. It has the most H-bonds, with interacting residues including GLU 1092, ASN 1108, TYR 1209, LYS 1211, and TRP 1212. The obtained statistical and numerical values from the proper visualizations figures (Figs. 1–6) and tables (Tables 1–5 and supplementary table) to make it clearly explained the metrics used to validate the performance of the computational approaches that predict pectolinarin will deliver a new medicine for the treatment of SARS-CoV-2 in the future.

Funding statement

Authors did not receive any specific grant from funding agencies from government and non-government agencies.

CRedit authorship contribution statement

Mukta Rani: Data curation, Formal analysis, Investigation, Validation, Visualization, Methodology, Resources, Writing – original draft. **Amit Kumar Sharma:** Conceptualization, Methodology, Investigation, Validation, Writing – original draft, Writing – review & editing. **R.S. Chouhan:** Writing – original draft. **Souvik Sur:** Formal analysis, Validation, Writing – original draft. **Rani Mansuri:** Writing – original draft. **Rajesh K. Singh:** Conceptualization, Writing – original draft, Writing – review & editing.

Declaration of competing interest

The authors declare that they have no known competing financial interests or personal relationships that could have appeared to influence the work reported in this paper.

Data availability

Data will be made available on request.

Acknowledgements

AKS would like to thank our Director, Prof. R. K. Dwivedi, FOE & CS, Teerthanker Mahaveer University, Moradabad and MR would like to thank the National Institute for Plant Biotechnology, Indian Council of Agricultural Research, Pusa Campus, New Delhi, for providing infrastructure and computer facilities.

Appendix A. Supplementary data

Supplementary data to this article can be found online at <https://doi.org/10.1016/j.crstbi.2023.100120>.

References

- Alzaabi, M.M., Hamdy, R., Ashmawy, N.S., et al., 2022. Flavonoids are promising safety therapy against COVID-19. *Phytochemistry Rev.* 21 (1), 291–312. <https://doi.org/10.1007/s11011-021-09759-z>.
- Ashour, H.M., Elkhatib, W.F., Rahman, M., Elshabrawy, H.A., 2020. Insights into the recent 2019 novel coronavirus (SARS-CoV-2) in light of past human coronavirus outbreaks. *Pathogens* 9 (3), 186–201. <https://doi.org/10.3390/pathogens9030186>.
- Bhattacharya, D., Nowotny, J., Cao, R., Cheng, J., 2016. 3Drefine: an interactive web server for efficient protein structure refinement. *Nucleic Acids Res.* 44 (W1), W406–W409. <https://doi.org/10.1093/nar/gkw336>.
- Burak, M., Imen, Y., 1999. Flavonoids and their antioxidant properties. *Turkiye Klin Tip Bil Derg* 19 (1), 296–304.
- Case, D.A., Cheatham, T.E., Darden, T., Gohlke, H., Luo, R., Merz Jr., M. K., Onufriev, A., Simmerling, C., Wang, B., Woods, R., 2005. The Amber biomolecular simulation programs. *J. Comput. Chem.* 26, 1668–1688. <https://doi.org/10.1002/jcc.20290>.
- Chen, D., Oezguen, N., Urvil, P., Ferguson, C., Dann, S.M., Savidge, T.C., 2016. Regulation of protein-ligand binding affinity by hydrogen bond pairing. *Sci. Adv.* 25 (2), e1501240 <https://doi.org/10.1126/sciadv.1501240>, 3.
- Cho, S., Lee, J., Lee, Y.K., Chung, M.J., Kwon, K.H., Lee, S., 2016. Determination of pectolarin in *Cirsium* spp. using HPLC/UV analysis. *J. Appl. Biol. Chem.* 59 (2), 107–112. <https://doi.org/10.3839/jabc.2016.020>.
- DeLano, W., 2002. The PyMOL Molecular Graphics System. DeLano Scientific, San Carlos, CA, USA.
- Eltayb, W.A., Abdalla, M., Rabie, A.M., 2023. Novel investigational anti-SARS-CoV-2 agent ensitrelvir “S-217622”: a very promising potential universal broad-spectrum antiviral at the therapeutic frontline of coronavirus species. *ACS Omega* 8 (6), 5234–5246. <https://doi.org/10.1021/acsomega.2c03881>.
- Fennell-Fezzie, R., Gradia, S.D., Akey, D., Berger, J.M., 2005. The MukF subunit of *Escherichia coli* condensin: architecture and functional relationship to kleisins. *EMBO J.* 1 (24), 1921–1930. <https://doi.org/10.1038/sj.emboj.7600680>.
- Forni, D., Cagliani, R., Clerici, M., Sironi, M., 2017. Molecular evolution of human coronavirus genomes. *Trends Microbiol.* 25 (1), 35–48. <https://doi.org/10.1016/j.tim.2016.09.001>.
- Groot, H.D., Rauen, U., 1998. Tissue injury by reactive oxygen species and the protective effects of flavonoids. *Fundam. Clin. Pharmacol.* 12 (3), 249–255. <https://doi.org/10.1111/j.1472-8206.1998.tb00951.x>.
- Hoffmann, M., Kleine-Weber, H., Schroeder, S., Kruger, N., Herrler, T., Erichsen, S., 2020. SARS-CoV-2 cell entry depends on ACE2 and TMPRSS2 and is blocked by a clinically proven protease inhibitor. *Cell* S0092, 30229–30234. <https://doi.org/10.1016/j.cell.2020.02.052>, 10.2174/1389557521666210401090028.
- Jo, S., Kim, S., Kim, D.Y., Kim, M.S., Shin, D.H., 2020. Flavonoids with inhibitory activity against SARS-CoV-2 3CLpro. *J. Enzym. Inhib. Med. Chem.* 35 (1), 1539–1544. <https://doi.org/10.1080/14756366.2020.1801672>.
- Kelley, L.A., Mezulis, S., Yates, C.M., Wass, M.N., Sternberg, M.J., 2015. The Phyre2 web portal for protein modeling, prediction and analysis. *Nat. Protoc.* 10 (6), 845–858. <https://doi.org/10.1038/nprot.2015.053>.
- Khan, N., Syed, D.N., Ahmad, N., Mukhtar, H., 2013. Fisetin: a dietary antioxidant for health promotion. *Antioxidants Redox Signal.* 19 (2), 151–162. <https://doi.org/10.1089/ars.2012.4901>.
- Laskowski, R.A., MacArthur, M.W., Moss, D.S., Thornton, J.M., 1993. PROCHECK: a program to check the stereochemical quality of protein structures. *J. Appl. Crystallogr.* 26 (2), 283–291. <https://doi.org/10.1107/S0021889892009944>.
- Li, F., 2016. Structure, function, and evolution of coronavirus spike proteins. *Annu Rev Virol* 29 (3), 237–261. <https://doi.org/10.1146/annurev-virology-110615-042301>.
- Li, F., Li, W., Farzan, M., Harrison, S.C., 2005. Structure of SARS coronavirus spike receptor-binding domain complexed with receptor. *Science* 309 (5742), 1864–1868. <https://doi.org/10.1126/science.1116480>.
- Lovell, S., Davis, I., Arendall, W., de Bakker, P., Word, J., Prisant, M., 2003. Structure validation by C-alpha geometry: phi, psi and C-beta deviation. *Proteins* 50, 437–450. <https://doi.org/10.1002/prot.10286>, 2003.
- Malashkevich, V.N., Chan, D.C., Chutkowski, C.T., Kim, P.S., 1998. Crystal structure of the simian immunodeficiency virus (SIV) gp41 core: conserved helical interactions underlie the broad inhibitory activity of gp41 peptides. *Proc. Natl. Acad. Sci. U.S.A.* 95, 9134–9139. <https://doi.org/10.1073/pnas.95.16.9134>.
- Mashiach, E., Schneidman-Duhovny, D., Andrusier, N., Nussinov, R., Wolfson, H.J., 2008. FireDock: a web server for fast interaction refinement in molecular docking. *Nucleic Acids Res.* 36 (Suppl. 1_2), W229–W232. <https://doi.org/10.1093/nar/gkn186>.
- Mehta, S., Sharma, A.K., Singh, R.K., 2021a. Advances in ethnobotany, synthetic phytochemistry and pharmacology of endangered herb *Picrorhiza kurroa* (Kutki): a comprehensive review (2010–2020). *Mini Rev. Med. Chem* 21 (19), 2976–2995.
- Mehta, S., Sharma, A.K., Singh, R.K., 2021b. Therapeutic journey of andrographis paniculata (Burm.f.) nees from natural to synthetic and nanoformulations. *Mini Rev. Med. Chem.* 21 (12), 1556–1577. <https://doi.org/10.2174/1389557521666210315162354>.
- Morozov, A.V., Kortemme, T., Tsemekhan, K., Baker, D., 2004. Close agreement between the orientation dependence of hydrogen bonds observed in protein structures and quantum mechanical calculations. *Proc. Natl. Acad. Sci. USA* 101 (18), 6946–6951. <https://doi.org/10.1073/pnas.030757810>.
- Nabavi, S.F., Braidji, N., Habtemariam, S., Orhan, I.E., Daglia, M., Manayi, A., 2015. Neuroprotective effects of chrysin: from chemistry to medicine. *Neurochem. Int.* 90, 224–231. <https://doi.org/10.1016/j.neuint.2015.09.006>.
- Narayana, K.R., Reddy, M.S., Chaluvadi, M., Krishna, D., 2001. Bioflavonoids classification, pharmacological, biochemical effects and therapeutic potential. *Indian J. Pharmacol.* 33 (1), 2–16. <https://doi.org/10.5530/ijper.53.1.3>.
- Rabie, A.M., 2021. Two antioxidant 2,5-disubstituted-1,3,4-oxadiazoles (CoVTris2020 and ChloViD2020): successful repurposing against COVID-19 as the first potent multitarget anti-SARS-CoV-2 drugs. *New J. Chem.* 45 (2), 761–771. <https://doi.org/10.1039/D0NJ03708G>.
- Rabie, A.M., 2022. New potential inhibitors of coronaviral main protease (CoV-mpro): strychnine bush, pineapple, and ginger could be natural enemies of COVID-19. *Int. J. Network. Commun.* 9 (3), 225–237. <https://doi.org/10.22034/ijnc.2022.3.10>.
- Rabie, A.M., Abdalla, M., 2022. Forodesine and riboprine exhibit strong anti-SARS-CoV-2 repurposing potential: *in silico* and *in vitro* studies. *ACS Bio Med Chem Au* 2 (6), 565–585. <https://doi.org/10.1021/acsbiochemau.2c00039>.
- Rabie, A.M., Abdel-Dayem, A.M., Abdalla, M., 2023. Promising experimental anti-SARS-CoV-2 agent “SL1-0197800”: the prospective universal inhibitory properties against the coming versions of the coronavirus. *ACS Omega* 8 (39), 35538–35554. <https://doi.org/10.1021/acsomega.2c08073>.
- Rani, M., Nischal, A., Sahoo, G.C., Khattri, S., 2013. Computational analysis of the 3-D structure of human GPR87 protein: implications for structure-based drug design. *Asian Pac. J. Cancer Prev. APJCP* 14 (12), 7473–7482. <https://doi.org/10.7314/APJCP.2013.14.12.7473>.
- Salentin, S., Schreiber, S., Haupt, V.J., Adasme, M.F., Schroeder, M., 2015. PLIP: fully automated protein–ligand interaction profiler. *Nucleic Acids Res.* 43 (W1), W443–W447. <https://doi.org/10.1093/nar/gkv315>.
- Salomon-Ferrer, R., Case, D.A., Walker, R.C., 2013. An overview of the Amber biomolecular simulation package. *WIREs Comput. Mol. Sci.* 3, 198–210. <https://doi.org/10.1002/wcms.1121>.
- Schneidman-Duhovny, D., Inbar, Y., Nussinov, R., Wolfson, H.J., 2005. PatchDock and SymmDock: servers for rigid and symmetric docking. *Nucleic Acids Res.* 33 (Suppl. 1_2), W363–W367. <https://doi.org/10.1093/nar/gki481>.
- Sharma, A.K., Gaur, K., Tiwari, R.K., Gaur, M.S., 2011. Computational interaction analysis of organophosphorus pesticides with different metabolic proteins in humans. *Journal of Biomedical Research* 25, 335–347. [https://doi.org/10.1016/S1674-8301\(11\)60045-6](https://doi.org/10.1016/S1674-8301(11)60045-6).
- Sheahan, T.P., Sims, A.C., Graham, R.L., Menachery, V.D., Gralinski, L.E., Case, J.B., 2017. Broad-spectrum antiviral GS-5734 inhibits both epidemic and zoonotic coronaviruses. *Sci. Transl. Med.* 9 (396), e3653–e3661. <https://doi.org/10.1126/scitranslmed.aal3653>.
- Singh, R.K., Prasad, D.N., Bhardwaj, T.R., 2013. Synthesis *in vitro/in vivo* evaluation and *in silico* physicochemical study of prodrug approach for brain targeting of alkylating agent. *Med. Chem. Res.* 22, 5324–5336. <https://doi.org/10.1007/s00044-013-0537-0>.

- Singh, R.K., Prasad, D.N., Bhardwaj, T.R., 2015. Synthesis, physicochemical properties and kinetic study of bis(2-chloroethyl)amine as cytotoxic agent for brain delivery. *Arab. J. Chem.* 8, 380–387. <https://doi.org/10.1016/j.arabjc.2012.11.005>.
- Tian, K., Kasavajhala, K., Belfon, L., Raguetta, H., Huang, A., Miguez, J., Bickel, Y., Wang, J., Pincay, Q., Wu, C., 2020. Simmerling. ff19SB: amino-acid-specific protein backbone parameters trained against quantum mechanics energy surfaces in solution. *J. Chem. Theor. Comput.* 16, 528–552. <https://doi.org/10.1021/acs.jctc.9b00591>.
- Tortorici, M.A., Veessler, D., 2019. Structural insights into coronavirus entry. *Adv. Virus Res.* 105, 93–116. <https://doi.org/10.1016/bs.aivir.2019.08.002>.
- Walls, A.C., Xiong, X., Park, Y.J., Tortorici, M.A., Snijder, J., Quispe, J., 2019. Unexpected receptor functional mimicry elucidates activation of coronavirus fusion. *Cell* 176 (5), 1026–1039. <https://doi.org/10.1016/j.cell.2018.12.028>.
- Walls, A.C., Park, Y.J., Tortorici, M.A., Wall, A., McGuire, A.T., Veessler, D., 2020. Structure, function, and antigenicity of the SARS-CoV-2 spike glycoprotein. *Cell* 181 (2), 281–292 e286. <https://doi.org/10.1016/j.cell.2020.02.058>.
- Waterhouse, A., Bertoni, M., Bienert, S., Studer, G., Tauriello, G., Gumienny, R., 2018. SWISS-MODEL: homology modelling of protein structures and complexes. *Nucleic Acids Res.* 46 (W1), W296–W303. <https://doi.org/10.1093/nar/gky427>.
- J. Parker, Bacteria, Editor(s): Sydney Brenner, Jefferey H. Miller, Encyclopedia of Genetics, Academic Press, 2001, Pages 146–151, ISBN 9780122270802, <https://doi.org/10.1006/rwgn.2001.0102>.
- Xia, E.Q., Deng, G.F., Guo, Y.J., Li, H.B., 2010. Biological activities of polyphenols from grapes. *Int. J. Mol. Sci.* 11 (2), 622–646. <https://doi.org/10.3390/ijms11020622>.
- Yang, J., Roy, A., Zhang, Y., 2013. Protein-ligand binding site recognition using complementary binding-specific substructure comparison and sequence profile alignment. *Bioinformatics* 15 (20), 2588–2595. <https://doi.org/10.1093/bioinformatics/btt447>, 29.
- Yang, J., Yan, R., Roy, A., Xu, D., Poisson, J., Zhang, Y., 2015. The I-TASSER Suite: protein structure and function prediction. *Nat. Methods* 12 (1), 7–8. <https://doi.org/10.1038/nmeth.3213>.
- Yang, H., Lou, C., Sun, L., Li, J., Cai, Y., Wang, Z., 2019. admetSAR 2.0: web-service for prediction and optimization of chemical ADMET properties. *Bioinformatics* 35 (6), 1067–1069. <https://doi.org/10.1093/bioinformatics/bty707>.
- Yuan, Y., Cao, D., Zhang, Y., Ma, J., Qi, J., Wang, Q., 2017. Cryo-EM structures of MERS-CoV and SARS-CoV spike glycoproteins reveal the dynamic receptor binding domains. *Nature Commun* 8 (1), 1–9. <https://doi.org/10.1038/ncomms15092>.
- WHO, Coronavirus Disease (COVID-19) Dashboard, <https://covid19.who.int>, 3 September 2020.